Proceedings of the ASME 2010 Summer Bioengineering Conference
SBC2010
June 16-19, 2010, Naples, Florida, USA

SBC2010-19336

PATIENT-SPECIFIC FINITE ELEMENT ANALYSIS OF CAROTID ARTERY STENTING

Michele Conti (1, 2), Ferdinando Auricchio (1), Gianluca De Santis (2), Matthieu De Beule (2), Benedict Verhegghe (2)

(1) Structural Mechanics Department,
Università degli Studi di Pavia,
Pavia, Italy

(2) bioMMeda-IBiTech,
Faculty of Engineering, Ghent University,
Ghent, Belgium

INTRODUCTION

At present, the clinical trend to treat peripheral atherosclerotic vessels, such as the carotid or the superficial femoral artery, is to apply percutaneous techniques using Nitinol self-expanding stents.

This class of stents addresses the biomechanical requirements (i.e. flexibility, kink resistance, etc.), but it has been observed that many of these stents implanted in peripheral vessels are fractured or have limited performance. Moreover, currently, many different stent designs are available on the rapidly growing dedicated market which, on the one hand, is enlarging the available interventional options but, on the other hand, is complicating the standardization of the treatment strategy thus relating the clinical success to the ability of the operator. Consequently, there is a significant need to relate the clinical outcomes to the device design as recently highlighted by some clinical experts (Stockx, 2006).

Although computational tools, such as Finite Element Analysis (FEA), are largely used to investigate coronary stenting (Auricchio et al., 2000; Lally et al., 2005; De Beule, 2009), few studies have been published on FEA of Carotid Artery Stenting (CAS) (Wu et al., 2007; Conti et al., 2009a, b).

In the present study, we propose the FEA of Nitinol stent deployment in a carotid artery (CA) model based on patient-specific geometrical data obtained from Computed Tomography Angiography (CTA). In particular, in this study, we focus on two stent models based on two commercially available designs, i.e. the open-cell ACCULINK stent (Abbott, Illinois, USA) - labeled as design A and the closed-cell XACT stent (Abbott, Illinois, USA) - labeled as design B. It has to be underlined that, in order to focus the comparison mainly on the design features, the same thickness of 0.24 mm is assumed for both designs.

MATERIALS AND METHODS

We process the DICOM CTA images of a stenosed carotid bifurcation of a 83 years-old male patient using Mimics v.13 (Materialise, Leuven, Belgium) generating a STL file defining the lumen profile. Then, we elaborate the STL file using pyFormex v.0.8 (http://pyformex.berlios.de/) to reconstruct the CA outer profile and to generate a high-quality, full hexahedral mesh with balanced resolution in each branch and minimal deformation for each element (De Santis et al., 2009) (see figure 1). We adopt a reconstruction strategy accounting for vessel tapering thus considering the wall thickness as a percentage (i.e., 30%) of the vessel radius. The vessel tissue is modeled as an isotropic hyperelastic material (Lally et al., 2005) and the density is assumed 1 g/cm^3. During the FEA of CAS, the stent deformation is driven by the catheter model and in particular the simulation consists of two main steps: 1) crimping and bending of the catheter while the contact between the stent and the vessel is deactivated; 2) gradually re-expansion of the catheter while the contact between the stent and the vessel is activated. We use Abaqus/Explicit as finite element solver since the numerical analysis is non-linear, involving large deformation and contact. The numerical results are post-processed to evaluate the impact of stent design on post-stenting vessel straightening (evaluating the tortuosity as proposed by Thomas et al., 2005) and lumen gain.

RESULTS AND DISCUSSION

Figure 2 illustrates the vessel, stent and catheter configuration during the CAS simulation for stent B. From the results reported in table 1, for the investigated anatomy, we speculate that: i) the stent B provides the best ICA lumen gain; ii) although the open-cell design A has a slightly minor impact than the design B on vessel tortuosity, both designs straighten the vessel considerably. Even though we consider a realistic carotid artery geometry assessed by in-vivo imaging (CTA), from a modeling point of view, the main limitations of the present study are related to: 1) the absence of the atherosclerotic plaque; 2) the lack of information on the actual wall thickness; 3) the isotropic response of the vessel tissue.

CONCLUSIONS

In the present study, we propose the FEA of stent deployment in a patient-specific CA model as a computational tool to compare different stent designs in the same vascular anatomy. Although the highlighted limitations, we believe that the present study represents a solid base for further developments aiming to define a reliable virtual procedure planning of CAS supporting, in the one hand, the assessment of procedure standardization, and, on the other hand, relating complex mechanical features of a given stent design to a given patient-specific anatomy. Clearly, due to the complexity of the system under investigation, the numerical results should be embedded in a broader process accounting for clinical and biological considerations where the surgeons experience has a primary role. Further studies will address the model validation comparing the numerical outcomes with both experimental tests (using a patient-specific silicon mock artery) and medical images (pre-, post-stenting and follow-up of a CAS procedure).

ACKNOWLEDGEMENT

The authors would acknowledge: Dr. R. Dore, Dr. A. Odero and Dr. S. Pirrelli of IRCCS Policlinico S. Matteo, Pavia, Italy for support on medical aspects related to the present work; Eng. D. Van Loo of UGent University, Belgium for micro-CT scanning of stent samples.

REFERENCES

Auricchio, F., Di Loreto, M., Sacco, E., 2000. Finite element analysis of a stenotic artery revascularization through stent insertion. Computer Methods in Biomechanics and Biomedical Engineering 0, 1–15.

Conti, M., Auricchio, F., De Beule, M., Verhegghe, B., 2009a. Numerical simulation of Nitinol peripheral stents: from laser-cutting to deployment in a patient specific anatomy. Proceeding of ESOMAT 2009 doi: 10.1051/esomat/200906008, 06008.

Conti, M., De Beule, M., Mortier, P., Van Loo, D., Verdonck, P., Vermassen, F., Segers, P., Auricchio, F., Verhegghe, B., 2009b. Nitinol Embolic Protection Filters: design investigation by Finite Element Analysis. Journal of Materials Engineering and Performance doi: 10.1007/s11665-009-9408-8.

De Beule, M., 2009. Biomechanical Modeling of Stents: Survey 1997-2007 in Advances in Biomedical Engineering. P. Verdonck (Elsevier).

De Santis, G., Mortier, P., De Beule, M., Taeymans, Y., Segers, P., Verdonck, P., Verhegghe, B., 2009. Parametric hexahedral patient-specific mesh generation from coronary angiography using pyformex. Proceedings of the ASME 2009 summer Bioengineering Conference (SBC2009).

Thomas, J., Antiga, L., Che, S., Milner, J., Hangan Steinman, D., Spence, J., Kutt, B., Steinman, D.A., 2005. Variation in the Carotid Bifurcation Geometry of Young Versus Older Adults: Implications for Geometric Risk of Atherosclerosis. Stroke 36, 2450–6.

Wu, W., Qi, M., Liu, X., Yang, D., Wang, W., 2007. Delivery and release of nitinol stent in carotid artery and their interactions: A finite element analysis. Journal of Biomechanics 40, 3034–3040.

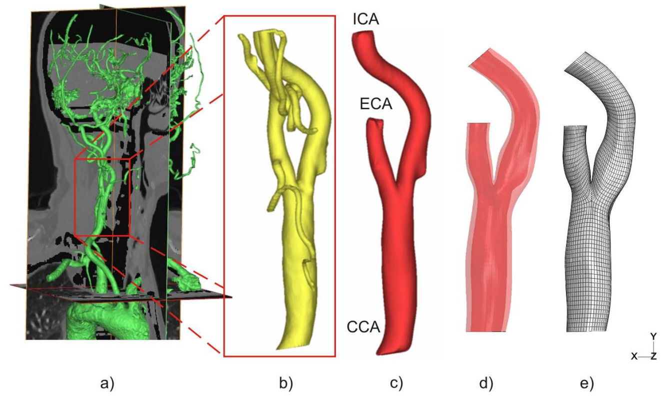

Figure 1. Patient-specific CA model: a) 3D reconstruction of vascular tree; b) lumen of CA bifurcation with also secondary branches; c) lumen of CA main branches (CCA: common carotid artery; ICA: internal carotid artery; ECA: external carotid artery); d) CA lumen (dark red) and reconstructed outer vessel wall profile (light red); e) hexahedral mesh.

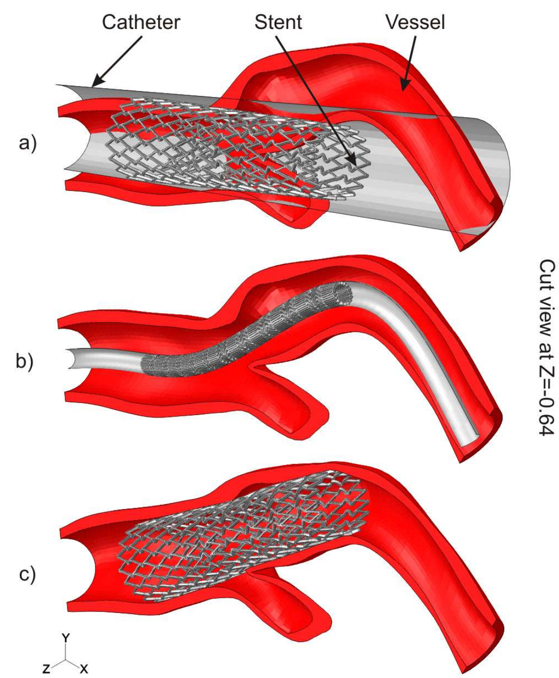

Figure 2. Simulation of stent implantation for stent B: a) starting configuration of the FE model; b) stent crimped in the delivery system; c) stent deployed in the vessel.

Table 1: Pre- and Post-stenting branch lumen and tortuosity.

	Pre-stenting	Post-stenting	
Stent Model		A	B
ICA lumen [mm^2]	18.0	26.4	30.1
ECA lumen [mm^2]	13.6	12.4	11.8
ICA lumen gain [%]	-	46.5	67.0
Tortuosity	0.029	0.013	0.011